The scattering map in the spatial Hill's problem

A. Delshams*, J.J. Masdemont†and P. Roldán‡

November 16, 2006

Abstract

We present a framework and methodology to compute the scattering map associated to heteroclinic trajectories in the spatial Hill's problem. The scattering map can be applied to design of zero-cost transfer trajectories in astrodynamics.

1 Introduction

The goal of this paper is to compute the scattering map associated to heteroclinic trajectories from the neighborhood of L_1 to the neighborhood of L_2 (or vice versa) in the spatial Hill's problem.

The planar Hill's problem was studied extensively by Simó and Stuchi in [22], where they already computed several homoclinic and heteroclinic connections. Recently, accurate numerical procedures have been developed to compute homoclinic and heteroclinic orbits in the spatial Hill's problem [13], [19].

The scattering map was first introduced in [6]. It plays a crucial part in the mechanism of diffusion described in [4]. Its properties have been studied extensively in [5].

In [2] we studied the scattering map in the planar restricted three body problemas a first step to understand it in the spatial problem. Compared with [2], the present paper is more complex, because one has to deal with manifolds two dimensions higher. This fact makes manifold intersections harder to compute and manifold tangencies harder to detect. On the other hand, going one degree of freedom higher gives room to trajectories connecting different invariant tori and to so-called Arnold's diffusion.

As an example application, consider a spacecraft orbiting in a given Lissajous orbit with small out-of-plane amplitude around L_1 in the Sun-Earth system. For some reason (for instance due to a contingency plan), we would like to have the spacecraft transfered to a Lissajous orbit around L_1 with large out-of-plane amplitude *at the minimum fuel cost*. Performing the transfer using classical maneuvers is expensive in terms of delta-v but, using heteroclinic connections and the scattering map, it can be performed at almost zero cost (see section 5.3). The main drawback is longer transfer times.

This paper presents a framework and methodology for the computation of scattering maps in the spatial Hill's problem. Moreover, the methodology can be

*<Amadeu.Delshams@upc.edu>
†<josep@barquins.upc.edu>
‡<Pablo.Roldan@upc.edu>, corresponding author

easily adapted to similar problems. The methodology is indebted to the work of C. Simó and his collaborators, who were the first to sistematically apply dinamical systems theory to space mission design. The series of volumes [12], [14], [10], [11] is a compendium of their work.

The main contributions of this paper are:

- Clarification of the relation of Lindstedt-Poincaré expansions to Birkhoff normal forms (section 3.2.1).
- Description of a method to compute heteroclinic trajectories from the normally hyperbolic invariant manifold of the equilibrium point L_i to that of L_j (section 4.2). Numerical results are given for Hill's problem.
- A method to compute the wave operators in Hill's problem. Semi-analitic formulas for the wave operators are given using Lindstedt-Poincaré variables (section 5.1).
- A method to determine heteroclinic channels in Hill's problem (section 5.2). Some heteroclinic channels are constructed explicitly for illustration.

Once the wave operators and heteroclinic channels are known, it is straightforward to compute the associated scattering maps (see section 5.3). In particular, we introduce a *reduced* form of the scattering map that captures all the information present in the usual scattering map in Hill's problem.

This paper does not describe in detail the possible uses of the scattering map in Hill's problem. However we present a simple application in section 5.3 for illustration. We plan to show some interesting applications in a future paper.

2 The spatial Hill's problem

Assume that two large bodies (for instance, the Sun and the Earth) follow circular orbits around their center of mass. The spatial restricted three body problem (RTBP for short) consists in describing the motion of a third body of negligible mass (for instance, the Moon) under the gravitational influence of the two massive bodies. Usually, the two large bodies are called "primaries". The one with larger mass $1-\mu$ is called P_1 and the one with smaller mass μ is called P_2.

The equations of motion of the third particle are given in [23], section 10.2. We denote (X, Y, Z) the position coordinates of the third particle. We remark that the motion of the third body is not constrained to the plane defined by the primaries.

Hill's problem is a limit version of the RTBP focusing on the neighborhood of the smallest primary, P_2 (see [23], [22]). The computations of heteroclinic trajectories in this paper are done using Hill's equations instead of RTBP equations, because they are simpler and they present a symmetry. Moreover, this allows us to compare results with [22] and [19]. The results can be extended to the RTBP for small values of the mass μ.

Hill's model can be obtained from the RTBP by a translation of the origin to the small primary followed by a $\mu^{1/3}$ rescaling:

$$X \to X\mu^{1/3} + \mu - 1, \quad Y \to Y\mu^{1/3}, \quad Z \to Z\mu^{1/3}.$$

Expanding the equations in powers of $\mu^{1/3}$ and considering only the dominant terms, one obtains Hill's limit:

$$\begin{aligned} \ddot{X} - 2\dot{Y} &= \frac{\partial \Omega}{\partial X} \\ \ddot{Y} + 2\dot{X} &= \frac{\partial \Omega}{\partial Y} \\ \ddot{Z} &= \frac{\partial \Omega}{\partial Z} \end{aligned}$$

where

$$\Omega(X, Y, Z) = \frac{3}{2}X^2 - \frac{1}{2}Z^2 + \frac{1}{\sqrt{X^2 + Y^2 + Z^2}}.$$

There exists an integral of this system, known as the Jacobian integral:

$$\dot{X}^2 + \dot{Y}^2 + \dot{Z}^2 = 2\Omega(X, Y, Z) - C, \tag{1}$$

where C is called the Jacobian constant.

Two of the collinear fixed points of the RTBP, L_1 and L_2, persist in Hill's problem. They are located symmetrically with respect to the $X = 0$ plane on the X axis, at a distance $\gamma = 3^{-1/3}$ of the small primary.

To focus on the neighborhood of one of the equilibrium points (L_1 or L_2), we shift the coordinate system to the equilibrium point and scale it so that the distance from the closest primary to the origin becomes one:

$$X = -\gamma\xi + \beta, \quad Y = -\gamma\eta, \quad Z = \gamma\zeta$$

where $\beta = \pm\gamma$, with the upper sign for L_1 and the lower one for L_2. In terms of these new variables, the equations of motion become (see [21]):

$$\begin{aligned} \ddot{\xi} - 2\dot{\eta} &= \frac{1}{\gamma^2}\frac{\partial \Omega_L}{\partial \xi}, \\ \ddot{\eta} + 2\dot{\xi} &= \frac{1}{\gamma^2}\frac{\partial \Omega_L}{\partial \eta}, \\ \ddot{\zeta} &= \frac{1}{\gamma^2}\frac{\partial \Omega_L}{\partial \zeta}, \end{aligned} \tag{2}$$

where

$$\Omega_L(\xi, \eta, \zeta) = \frac{3\gamma^2}{2}(\xi + 1)^2 - \frac{\gamma^2}{2}\zeta^2 + \frac{1}{\gamma\sqrt{(\xi + 1)^2 + \eta^2 + \zeta^2}}.$$

The Jacobian integral is again

$$\dot{\xi}^2 + \dot{\eta}^2 + \dot{\zeta}^2 = 2\Omega_L(\xi, \eta, \zeta) - C_L,$$

where $C = \gamma^2 C_L$.

Introducing momenta in this rotating system

$$p_\xi = \dot{\xi} - \eta, \qquad p_\eta = \dot{\eta} + \xi, \qquad p_\zeta = \zeta,$$

a time-independent Hamiltonian function can be obtained:

$$\begin{aligned} H_L(\xi,\eta,\zeta,p_\xi,p_\eta,p_\zeta) = \frac{1}{2}\left(p_\xi^2+p_\eta^2+p_\zeta^2\right) + \eta p_\xi - \xi p_\eta \\ + \frac{1}{2}\left(\xi^2+\eta^2\right) - \frac{1}{\gamma^2}\Omega_L(\xi,\eta,\zeta). \end{aligned} \tag{3}$$

It is an integral of the system closely related to the Jacobian integral. In fact, $C_L = -2H_L$.

We will denote (M, φ^t) the phase space and the flow associated to (3).

3 Representation of the dynamics near L_1 and L_2

This section gives a description of the dynamics in the neighborhood of an equilibrium point ($L = L_1$ or L_2) using a Lindstedt-Poincaré procedure.

The Lindstedt-Poincaré procedure is analogous to a Birkhoff normal form, but without first diagonalizing the linear part of the equations. It produces an integrable approximation to the dynamics, with uncoupled elliptic and hyperbolic behaviour and the center part arranged as a rotation on the torus. Hence, it gives a representation of the invariant tori present in the center manifold, and associated stable and unstable manifolds. However, the representation is only valid in a small region around L due to small divisors. An advantage of the Lindstedt-Poincaré procedure with respect to normal forms is that it works with the original coordinates, and avoids a costly diagonalizing transformation.

For the numerical method used in section 4 to compute $L_i - L_j$ heteroclinic trajectories, it is necessary to work with the invariant tori around L_j, so we will use a Lindstedt-Poincaré representation, and restrict ourselves to the region where it is valid.

From the point of view of the scattering map, the important point is that the procedure is able to uncouple the center and hyperbolic directions, giving a local description of the stable and unstable manifolds' foliation (25). In this sense, we could have used a "reduction to center manifold" type of normal form instead of a Lindstedt-Poincaré or Birkhoff normal form. A detailed exposition of the "reduction to center manifold" procedure can be found in [18] or [10].

In this paper, we will simply use Lindstedt-Poincaré and normal form expansions without explaining how these expansions can be computed. For a justification of the expansions and details about their computation, we refer to [10], [18], [19], and references therein.

An important idea in dynamical systems is to identify certain sets of solutions with similar dynamical properties as invariant manifolds organizing the phase space. We summarize the local invariant manifolds present near the fixed point L of the spatial Hill's problem. We use truncated series to represent the manifolds, which gives a good numerical approximation to the exact manifolds.

3.1 Normal form expansions

The general idea behind normal forms is to simplify the Taylor expansion of the Hamiltonian around an equilibrium point using canonical changes of variables.

There are several types of normal forms, depending on the kind of transformations allowed and the "simple" form one puts the system into.

Let us briefly review the Birkhoff normal form procedure. For details see [17], for instance.

The Hamiltonian $H = H_L$ is expanded in power series using the Legendre polynomials, P_n:

$$H(\xi,\eta,\zeta,p_\xi,p_\eta,p_\zeta) = \sigma + \frac{1}{2}\left(p_\xi^2+p_\eta^2+p_\zeta^2\right) + \eta p_\xi - \xi p_\eta - \sum_{n\geq 2} c_n \rho^n P_n\left(\frac{\xi}{\rho}\right), \quad (4)$$

where $\rho^2 = \xi^2+\eta^2+\zeta^2$, $c_2 = 4$, $c_n = (\pm 1)^n 3 \quad n \geq 3$, and $\sigma = -\frac{9}{2}$.

Consider the second-order part of the Hamiltonian:

$$H_2(\xi,\eta,\zeta,p_\xi,p_\eta,p_\zeta) = \frac{1}{2}\left(p_\xi^2+p_\eta^2+p_\zeta^2\right) + \eta p_\xi - \xi p_\eta - c_2\xi^2 + \frac{c_2}{2}\eta^2 + \frac{c_2}{2}\zeta^2.$$

Let A be the linearization of the flow around the origin, i.e. $A = J\nabla H_2(0)$. The characteristic roots of A are two real roots of opposite sign, $\pm\lambda_0$, and two pairs of imaginary roots of opposite sign, $\pm i\omega_0$ and $\pm i\nu_0$, with

$$\lambda_0 = \sqrt{\frac{c_2 - 2 + \sqrt{9c_2^2-8c_2}}{2}}, \qquad \omega_0 = \sqrt{\frac{2 - c_2 + \sqrt{9c_2^2-8c_2}}{2}}, \qquad \nu_0 = \sqrt{c_2}.$$

Therefore, the equilibrium point L is of the type saddle $\times$ center $\times$ center.

As a preliminary step, diagonalize the linear part of the equations of motion, or equivalently, simplify the second-order part H_2 of the Hamiltonian.

Use first a linear symplectic change of coordinates

$$x \to Cx$$

where $x = (\xi,\eta,\zeta,p_\xi,p_\eta,p_\zeta)$. The matrix C is given explicitly in [19], section 4. Then, H_2 takes the form

$$H_2(\xi,\eta,\zeta,p_\xi,p_\eta,p_\zeta) = \lambda_0\xi p_\xi + \frac{\omega_0}{2}(\eta^2+p_\eta^2) + \frac{\nu_0}{2}(\zeta^2+p_\zeta^2).$$

Introduce then complex variables

$$\begin{pmatrix} q_2 \\ p_2 \end{pmatrix} = \frac{1}{\sqrt{2}}\begin{pmatrix} 1 & -i \\ -i & 1 \end{pmatrix}\begin{pmatrix} \eta \\ p_\eta \end{pmatrix}, \qquad \begin{pmatrix} q_3 \\ p_3 \end{pmatrix} = \frac{1}{\sqrt{2}}\begin{pmatrix} 1 & -i \\ -i & 1 \end{pmatrix}\begin{pmatrix} \zeta \\ p_\zeta \end{pmatrix} \quad (5)$$

and $\begin{pmatrix} q_1 \\ p_1 \end{pmatrix} = \begin{pmatrix} \xi \\ p_\xi \end{pmatrix}$ to complete the diagonalization of the linear part of the differential equations, which puts the Hamiltonian in the form

$$H_2(q_1,q_2,q_3,p_1,p_2,p_3) = \lambda_0 q_1 p_1 + i\omega_0 q_2 p_2 + i\nu_0 q_3 p_3. \quad (6)$$

Remark 1. We call attention to the fact that this diagonalizing transformation is nontrivial and very useful. The Lindstedt-Poincaré procedure avoids this preliminary tranformation at the expense of complicating the normalization procedure, and the final expansion is less compact than a Birkhoff normal form solution (compare equations (13) and (15)).

Next we arrange the nonlinear part of the differential equations. For economy, let us use multiindex notation: $q = (q_1, q_2, q_3)$, $q^i = (q_1^{i_1}, q_2^{i_2}, q_3^{i_3})$, $|i| = i_1 + i_2 + i_3$. Substituting the linearizing change of variables in the expansion (4) gives

$$H(q,p) = \sum_{n\geq 2} H_n(q,p), \quad H_n = \sum_{|i|+|j|=n} h_{ij} q^i p^j, \tag{7}$$

where h_{ij} are complex coefficients, and H_2 is given in (6).

The Birkhoff normal form procedure cancels all nonresonant terms of the Hamiltonian up to a certain degree N. One performs successive canonical transformations of the Hamiltonian (7) to obtain

$$H(q,p) = H_{\mathrm{B}}(q,p) + R(q,p),$$

where H_{B} is a degree N polynomial in Birkhoff normal form

$$H_{\mathrm{B}} = \lambda_0 q_1 p_1 + i\omega_0 q_2 p_2 + i\nu_0 q_3 p_3 + \hat{H}(q_1 p_1, q_2 p_2, q_3 p_3), \tag{8}$$

and R is a reminder of order $N+1$ in the variables. Introduce the variables $I_1 = q_1 p_1, I_2 = q_2 p_3, I_3 = q_3 p_3$ with associated canonical pairs $\varphi_1, \varphi_2, \varphi_3$. Notice that I_1, I_2, I_3 are first integrals of H_{B}:

$$\begin{aligned}
\dot{I}_1 &= \dot{I}_2 = \dot{I}_3 = 0 \\
\dot{\varphi_1} &= \frac{\partial H_{\mathrm{B}}}{\partial I_1} = \lambda_0 + \frac{\partial \hat{H}}{\partial I_1}(I_1^0, I_2^0, I_3^0) \\
\dot{\varphi_2} &= \frac{\partial H_{\mathrm{B}}}{\partial I_2} = i\omega_0 + \frac{\partial \hat{H}}{\partial I_2}(I_1^0, I_2^0, I_3^0) \\
\dot{\varphi_3} &= \frac{\partial H_{\mathrm{B}}}{\partial I_3} = i\nu_0 + \frac{\partial \hat{H}}{\partial I_3}(I_1^0, I_2^0, I_3^0).
\end{aligned} \tag{9}$$

where $(I_1^0, I_2^0, I_3^0) = (I_1(0), I_2(0), I_3(0))$. Therefore the Birkhoff normal form of degree N is integrable. The right-hand side is constant: it only depends on I_1, I_2, I_3. Introduce the frequency series

$$\begin{aligned}
\lambda &= \lambda_0 + \frac{\partial \hat{H}}{\partial I_1}(I_1^0, I_2^0, I_3^0) = \sum_{ikm} \lambda_{ikm} (q_1^0 p_1^0)^i (I_2^0)^k (I_3^0)^m \\
\omega &= \omega_0 + \frac{\partial \hat{H}}{\partial I_2}(I_1^0, I_2^0, I_3^0) = \sum_{ikm} \omega_{ikm} (q_1^0 p_1^0)^i (I_2^0)^k (I_3^0)^m \\
\nu &= \nu_0 + \frac{\partial \hat{H}}{\partial I_3}(I_1^0, I_2^0, I_3^0) = \sum_{ikm} \nu_{ikm} (q_1^0 p_1^0)^i (I_2^0)^k (I_3^0)^m.
\end{aligned} \tag{10}$$

where $(q_1^0, p_1^0) = (q_1(0), p_1(0))$.

We may realify the normalized Hamiltonian (8) using the inverse of the previous complexifying transformation (5) to obtain

$$H_{\mathrm{B}}(\xi, p_\xi, \eta, p_\eta, \zeta, p_\zeta) = \lambda_0 \xi p_\xi + \frac{\omega_0}{2}(\eta^2 + p_\eta^2) + \frac{\nu_0}{2}(\zeta^2 + p_\zeta^2) + \hat{H}(\xi p_\xi, \eta p_\eta, \zeta p_\zeta). \tag{11}$$

The corresponding Hamiltonian equations are

$$\dot{\xi} = \lambda\xi \qquad \dot{p_\xi} = -\lambda p_\xi \tag{12a}$$
$$\dot{\eta} = \omega p_\eta \qquad \dot{p_\eta} = -\omega\eta \tag{12b}$$
$$\dot{\zeta} = \nu p_\zeta \qquad \dot{p_\zeta} = -\nu\zeta \tag{12c}$$

with solution

$$\xi(t) = q_1^0 e^{\lambda t} \qquad p_\xi(t) = p_1^0 e^{-\lambda t} \tag{13a}$$
$$\eta(t) = I_2^0 \cos(\omega t + \varphi_2^0) \qquad p_\eta(t) = -I_2^0 \sin(\omega t + \varphi_2^0) \tag{13b}$$
$$\zeta(t) = I_3^0 \cos(\nu t + \varphi_3^0) \qquad p_\zeta(t) = -I_3^0 \sin(\nu t + \varphi_3^0), \tag{13c}$$

where

$$q_1^0 = \xi(0) \qquad p_1^0 = p_\xi(0)$$
$$I_2^0 = I_2(0) \qquad \varphi_2^0 = \varphi_2(0)$$
$$I_3^0 = I_3(0) \qquad \varphi_3^0 = \varphi_3(0).$$

In the normalization process there appear small divisors, which makes divergence of the process noticeable outside a small neighborhood V_{B} of the equilibrium point.

The Birkhoff normal form is equivalent to a Lindstedt-Poincaré expansion, as will be explained in section 3.2.1.

3.2 Lindstedt-Poincaré expansions

Consider first the linearization of the equations of motion (2) obtained by expanding the function Ω_L around the origin (equilibrium point) and neglecting terms of order 2 and higher in ξ, η and ζ:

$$\ddot{\xi} - 2\dot{\eta} = (1 + 2c_2)\xi$$
$$\ddot{\eta} + 2\dot{\xi} = (1 - c_2)\eta$$
$$\ddot{\zeta} = -c_2\zeta,$$

where $c_2 = 4$ for Hill's problem. (See [19] for details of the computation).

Recall that the eigenvalues of the linearized equations are $\pm\lambda_0$, $\pm i\omega_0$ and $\pm i\nu_0$. The solution of the linearized equations is

$$\xi(t) = \alpha_1 e^{\lambda_0 t} + \alpha_2 e^{-\lambda_0 t} + \alpha_3 \cos(\omega_0 t + \phi_1), \tag{14a}$$
$$\eta(t) = k_2\alpha_1 e^{\lambda_0 t} - k_2\alpha_2 e^{-\lambda_0 t} + k_1\alpha_3 \sin(\omega_0 t + \phi_1), \tag{14b}$$
$$\zeta(t) = \alpha_4 \cos(\nu_0 t + \phi_2), \tag{14c}$$

where $\alpha_1, \alpha_2, \alpha_3, \alpha_4, \phi_1, \phi_2$ are independent coefficients that can be completely determined from the initial conditions $\xi(t_0), \eta(t_0), \zeta(t_0), \dot{\xi}(t_0), \dot{\eta}(t_0), \dot{\zeta}(t_0)$, and k_1, k_2 are constant:

$$k_1 = -\frac{\omega_0^2 + 1 + 2c_2}{2\omega_0}, \qquad k_2 = \frac{\lambda_0^2 - 1 - 2c_2}{2\lambda_0}.$$

Note that the coefficients α_1 and α_2 are associated with the real exponents λ_0 and $-\lambda_0$, so the first term in the right hand side of expressions (14a) and (14b) has exponential growth, and the second term has exponential decay with time.

Selecting an initial condition

$$x_0 = (\xi_0, \eta_0, \zeta_0, \dot{\xi}_0, \dot{\eta_0}, \dot{\zeta}_0) = \Big(\xi(t_0), \eta(t_0), \zeta(t_0), \dot{\xi}(t_0), \dot{\eta}(t_0), \dot{\zeta}(t_0)\Big)$$

such that $\alpha_1 = \alpha_2 = 0$ yields a particular solution consisting of an elliptic motion in the ξ, η plane ("in-plane" component of the motion) and an uncoupled oscillation in the ζ direction ("out-of-plane" component). These bounded solutions may be periodic (if ν_0 and ω_0 are commensurable) or quasi-periodic. Each of these orbits, usually called Lissajous orbits, lies on a two-dimensional torus T_{α_3,α_4} characterized by the amplitudes α_3 and α_4, and parametrized by the angles $\theta_1 = \omega_0 t + \phi_1$ and $\theta_2 = \nu_0 t + \phi_2$.

Selecting initial coditions corresponding to $\alpha_3 = \alpha_4 = 0$ reduces to a saddle phase portrait in the ξ, η plane.

Combinations of these two cases give rise to solutions having both elliptic and hyperbolic behaviour. In particular, one can see directly from (14) that selecting an initial condition x_0 corresponding to $\alpha_1 = 0$ and $\alpha_2 \neq 0$ gives a solution tending to a Lissajous orbit as $t \to \infty$, i.e. the orbit of x_0 belongs to the stable manifold of the torus T_{α_3,α_4}. Notice that the stable manifold is actually composed of all such orbits. Similarly, if x_0 corresponds to $\alpha_1 \neq 0$ and $\alpha_2 = 0$, then the orbit of x_0 belongs to the unstable manifold of T_{α_3,α_4}.

Of course, the solutions discussed above are only valid for the linearized problem. However, in [19] it is shown that solutions of the exact problem can be well approximated in a neighborhood V_{LP} of the equilibrium point by a truncated series of the form

$$\begin{aligned}
\xi(t) &= \sum e^{(i-j)\lambda t} \left[\xi^{pq}_{ijkm} \cos\left(p\theta_1 + q\theta_2\right) + \bar{\xi}^{pq}_{ijkm} \sin(p\theta_1 + q\theta_2)\right] \alpha_1^i \alpha_2^j \alpha_3^k \alpha_4^m \\
\eta(t) &= \sum e^{(i-j)\lambda t} \left[\eta^{pq}_{ijkm} \cos(p\theta_1 + q\theta_2) + \bar{\eta}^{pq}_{ijkm} \sin(p\theta_1 + q\theta_2)\right] \alpha_1^i \alpha_2^j \alpha_3^k \alpha_4^m \qquad (15) \\
\zeta(t) &= \sum e^{(i-j)\lambda t} \left[\zeta^{pq}_{ijkm} \cos(p\theta_1 + q\theta_2) + \bar{\zeta}^{pq}_{ijkm} \sin(p\theta_1 + q\theta_2)\right] \alpha_1^i \alpha_2^j \alpha_3^k \alpha_4^m
\end{aligned}$$

where $\alpha_1, \alpha_2, \alpha_3, \alpha_4$ are constant,

$$\theta_1(t) = \omega t + \phi_1, \qquad \theta_2(t) = \nu t + \phi_2,$$

and

$$\begin{aligned}
\lambda &= \sum \lambda_{ikm} \left(\alpha_1 \alpha_2\right)^i \alpha_3^k \alpha_4^m \\
\omega &= \sum \omega_{ikm} \left(\alpha_1 \alpha_2\right)^i \alpha_3^k \alpha_4^m \\
\nu &= \sum \nu_{ikm} \left(\alpha_1 \alpha_2\right)^i \alpha_3^k \alpha_4^m .
\end{aligned}$$

Summation is extended over all $i, j, k, m \in \mathbb{N}$ and $p, q \in \mathbb{Z}$. Compare with (9), (10).

By construction, the coefficients α_i and ϕ_i parametrize families of solutions of the nonlinear problem analogous to those families just discussed of the linear problem. Selecting an initial condition such that $\alpha_1 = \alpha_2 = 0$ in (15) yields a bounded solution with associated invariant torus $\mathcal{T}_{\alpha_3,\alpha_4} = \mathcal{T}_{\alpha_3,\alpha_4}(\theta_1, \theta_2)$. If

$\alpha_1 = 0$ and $\alpha_2 \neq 0$, one obtains a solution in the stable manifold of $\mathcal{T}_{\alpha_3,\alpha_4}$, and if $\alpha_1 \neq 0$ and $\alpha_2 = 0$, a solution in the unstable manifold.

Let $M_{\mathrm{LP}} = \mathbb{R}^4 \times \mathbb{T}^2$ denote the space of Lindstedt-Poincaré coefficients. Let now

$$K\colon M_{\mathrm{LP}} \to M \tag{16}$$

denote the Lindstedt-Poincaré transformation that, given $t = t_0$, takes the coefficients $(\alpha_1, \alpha_2, \alpha_3, \alpha_4, \phi_1, \phi_2)$ to Hill's variables $(\xi, \eta, \zeta, \dot{\xi}, \dot{\eta}, \dot{\zeta})$ through expression (15). Consider the set

$$N = \{(\alpha_1, \alpha_2, \alpha_3, \alpha_4, \phi_1, \phi_2) \in M_{\mathrm{LP}}\colon \alpha_1 = \alpha_2 = 0\} \cap V_{\mathrm{LP}}. \tag{17}$$

When using Lindstedt-Poincaré coordinates, we will write a point in this manifold as $x = (\alpha_3, \alpha_4, \phi_1, \phi_2) \in N$. The restriction $k = K|_N$, $k\colon N \to M$ gives the Lindstedt-Poincaré parametrization of the (approximate) local center manifold

$$\Lambda = \{k(\alpha_3, \alpha_4, \phi_1, \phi_2)\colon (\alpha_3, \alpha_4, \phi_1, \phi_2) \in N\}\,.$$

For fixed $\bar{\alpha_3}, \bar{\alpha_4}$, the associated invariant torus is given in Lindstedt-Poincaré coordinates by

$$\mathcal{T}_{\bar{\alpha_3},\bar{\alpha_4}} = \{k(x)\colon x = (\alpha_3, \alpha_4, \phi_1, \phi_2) \in N,\ \alpha_3 = \bar{\alpha_3},\ \alpha_4 = \bar{\alpha_4}\}\,.$$

We will write a point in an invariant torus as $x = k(\phi_1, \phi_2) \in \mathcal{T}_{\bar{\alpha_3},\bar{\alpha_4}}$.

The (approximate) local stable (resp. unstable) manifold of a torus is given by

$$W^s_{\mathrm{loc}}\left(\mathcal{T}_{\bar{\alpha_3},\bar{\alpha_4}}\right) = \{k(x)\colon x = (0, \alpha_2, \bar{\alpha_3}, \bar{\alpha_4}, \phi_1, \phi_2) \in M_{\mathrm{LP}}\} \cap V_{\mathrm{LP}} \tag{18a}$$

$$W^u_{\mathrm{loc}}\left(\mathcal{T}_{\bar{\alpha_3},\bar{\alpha_4}}\right) = \{k(x)\colon x = (\alpha_1, 0, \bar{\alpha_3}, \bar{\alpha_4}, \phi_1, \phi_2) \in M_{\mathrm{LP}}\} \cap V_{\mathrm{LP}}. \tag{18b}$$

They extend to global stable and unstable manifolds $W^s_{\mathcal{T}_{\bar{\alpha_3},\bar{\alpha_4}}}, W^u_{\mathcal{T}_{\bar{\alpha_3},\bar{\alpha_4}}}$.

When the out-of-plane amplitude α_4 is zero, the torus $\mathcal{T}_{\alpha_3,0}$ naturally corresponds to a periodic Lyapunov orbit in the planar RTBP. It is well known that the amplitude of this periodic orbit increases as the Jacobi constant C decreases, starting at $C_{max} = C_1$ or C_2, the value at the equilibrium point $L = L_1$ or L_2 (see [23]). Due to the local character of the expansions of the solutions, we will restrict the maximum amplitude value for α_3 when $\alpha_4 = 0$, $\alpha_3 \in [0, \alpha_3^*]$ or equivalently the minimum energy value,

$$C \in [C_{min}, C_{max}]\,.$$

Notice that the local center manifold of L is the union of all tori "close" to L:

$$\Lambda = \bigcup_{C(\alpha_3,\alpha_4)\in[C_{min},C_{max}]} \mathcal{T}_{\alpha_3,\alpha_4}.$$

It is a biparametric (α_3, α_4) family of invariant tori.

Remark that the Lindstedt-Poincaré or Birkhoff normal form process is known to be divergent (see [18]), and the transformation (15) is only computed up to a finite degree. Nonetheless the original flow (generated by (2)) and the approximate flow (15) are locally conjugate up to a very small numerical error, because the divergence is not too fast, and the conjugacy is computed up to high order. Hence Λ is a good approximation to the exact local center manifold

(that of the original equations of motion (2)). In fact, the exact center manifold is practically full of invariant tori; the measure of the set of points between tori is exponentially small (see [7]).

Sometimes it will be convenient to consider the restriction of the center manifold to a given level of energy. Let M^c denote the points of the phase space M with Jacobian constant $C = c$ as defined in (1). Let us fix $c \in [C_{min}, C_{max}]$ and consider the set $\Lambda^c = \Lambda \cap M^c$,

$$\Lambda^c = \bigcup_{C(\alpha_3,\alpha_4)=c} \mathcal{T}_{\alpha_3,\alpha_4}.$$

Given that the amplitudes α_3, α_4 are related through the Jacobian integral, this is a one-parametric family of invariant tori whose extremal degenerate tori $\mathcal{T}_{\alpha_3,0}$ and $\mathcal{T}_{0,\alpha_4}$ are periodic orbits. These are usually called planar and vertical Lyapunov orbits in the literature. Let us call $\alpha \in [\alpha_{min}, \alpha_{max}]$ the parameter indexing the restricted center manifold,

$$\Lambda^c = \bigcup_{\alpha\in[\alpha_{min},\alpha_{max}]} \mathcal{T}_{\alpha}. \tag{19}$$

For instance, one could take $\alpha = \alpha_4$ as the parameter, which varies between 0 and a certain maximum amplitude. Topologically, the manifold Λ^c is the 3-sphere S^3 (see [3]).

3.2.1 Relation to Birkhoff normal form

We have seen that one can transform the original Hamiltonian (4) into its real Birkhoff normal form (11) through a series of canonical changes of variables. Let us denote $h\colon M_{\rm B} \to M$ the total transformation that takes the real Birkhoff normal form variables $\bar{x} = (\bar{\xi}, \bar{\eta}, \bar{\zeta}, \bar{p_\xi}, \bar{p_\eta}, \bar{p_\zeta})$ to the original variables $x = (\xi, \eta, \zeta, p_\xi, p_\eta, p_\zeta)$.

Write now the old variables in terms of the new ones. For instance,

$$\xi = h^1\left(\bar{\xi}, \bar{\eta}, \bar{\zeta}, \bar{p_\xi}, \bar{p_\eta}, \bar{p_\zeta}\right) = \sum_l h_l^1 \bar{\xi}^i \bar{p_\xi}^j \bar{\eta}^{k_1} \bar{p_\eta}^{k_2} \bar{\zeta}^{m_1} \bar{p_\zeta}^{m_2}$$

where h^1 is the first component of h, $l = (i, j, k_1, k_2, m_1, m_2)$ is a multiindex, and h_l^1 are complex coefficients. There are similar expressions for the other variables $\eta, \zeta, p_\xi, p_\eta, p_\zeta$.

Substitute the solution (13) to the Birkhoff normal form for $\bar{\xi}, \bar{\eta}, \bar{\zeta}, \bar{p_\xi}, \bar{p_\eta}, \bar{p_\zeta}$,

$$\begin{aligned}
\xi &= \sum_l h_l^1 \left(q_1^0 e^{\lambda t}\right)^i \left(p_1^0 e^{-\lambda t}\right)^j \left(I_2^0 \cos(\omega t + \varphi_2^0)\right)^{k_1} \left(-I_2^0 \sin(\omega t + \varphi_2^0)\right)^{k_2} \\
&\left(I_3^0 \cos(\nu t + \varphi_3^0)\right)^{m_1} \left(-I_3^0 \sin(\nu t + \varphi_3^0)\right)^{m_2} \\
&= \sum_l e^{(i-j)\lambda t} \left[h_l^1 \left(\cos(\omega t + \varphi_2^0)\right)^{k_1} \left(-\sin(\omega t + \varphi_2^0)\right)^{k_2} \left(\cos(\nu t + \varphi_3^0)\right)^{m_1} \left(-\sin(\nu t + \varphi_3^0)\right)^{m_2}\right] \\
&\left({q_1}^0\right)^i \left(p_1^0\right)^j \left(I_2^0\right)^k \left(I_3^0\right)^m,
\end{aligned}$$

where $k = k_1 + k_2$ and $m = m_1 + m_2$. Writting the product inside brackets as

a trigonometric series, and identifying

$$\alpha_1 = q_1^0 \qquad \alpha_2 = p_1^0 \tag{20a}$$
$$\alpha_3 = I_2^0 \qquad \alpha_4 = I_3^0 \tag{20b}$$
$$\phi_1 = \varphi_2^0 \qquad \phi_2 = \varphi_3^0 \tag{20c}$$

or equivalently

$$q_1(t) = \alpha_1 e^{\lambda t} \qquad p_1(t) = \alpha_2 e^{-\lambda t} \tag{21a}$$
$$I_2(t) = \alpha_3 \qquad I_3(t) = \alpha_4 \tag{21b}$$
$$\varphi_2(t) = \omega t + \phi_1 \qquad \varphi_3(t) = \nu t + \phi_2, \tag{21c}$$

one obtains precisely the Lindstedt-Poincaré series (15).

Indeed, the Lindstedt-Poincaré expansion (15) is just the solution (written in the original coordinates) to the Birkhoff normal form equations (12). Hence the task to find the coefficients $(\xi^{pq}_{ijkm}, \bar{\xi}^{pq}_{ijkm})$ that compose the Lindstedt-Poincaré expansion is equivalent to finding the coefficients h^1_l of the Birkhoff normal form transformation.

Moreover, we stress the meaning of Lindstedt-Poincaré coefficients $(\alpha_1, \alpha_2, \alpha_3, \alpha_4, \phi_1, \phi_2)$ as initial conditions for the Birkhoff normal form solution, as (20) shows.

We will denote $(M_{\text{LP}}, \varphi^t_{\text{LP}})$ the phase space and flow associated to the motion of $(q_1, p_1, I_2, I_3, \varphi_2, \varphi_3)$ given by equations (21).

3.3 Normally hyperbolic invariant manifolds

Loosely speaking, the flow φ^t is normally hyperbolic at Λ provided $\Lambda \subset M$ is a compact invariant submanifold for φ^t, the flow is hyperbolic within the normal bundle to Λ, and the rate of contraction towards Λ in the stable and unstable directions is stronger than any possible contraction within Λ. The precise definition of a normally hyperbolic invariant manifold is given for instance in [8], [9], [16], [15], [20] or [5].

Recall that the stable (resp. unstable) manifold of a normally hyperbolic invariant manifold Λ is defined as

$$W^s_\Lambda = \left\{x \in M \mid \text{dist}\left(\varphi^t(x), \Lambda\right) \leq C_x e^{-\lambda t}, \quad t \geq 0\right\}$$
$$W^u_\Lambda = \left\{x \in M \mid \text{dist}\left(\varphi^t(x), \Lambda\right) \leq C_x e^{-\lambda |t|}, \quad t \leq 0\right\}$$

for some constants C_x and $\lambda \geq 0$. The stable (resp. unstable) manifold of a point $x \in \Lambda$ is defined as

$$W^s_x = \left\{y \in M \mid \text{dist}\left(\varphi^t(x), \varphi^t(y)\right) \leq C_{x,y} e^{-\lambda t}, \quad t \geq 0\right\}$$
$$W^u_x = \left\{y \in M \mid \text{dist}\left(\varphi^t(x), \varphi^t(y)\right) \leq C_{x,y} e^{-\lambda |t|}, \quad t \leq 0\right\}.$$

Normal hyperbolicity has important consequences. Namely, it guarantees that the invariant manifold Λ persists under small perturbations of the flow. It also gives a foliation for the stable and unstable manifolds of Λ; this fact will be used in section 5.1.

We proceed to discuss normally hyperbolic invariant manifolds in Hill's problem. It is straightforward to check from expression (21) that the stable (resp.

unstable) manifold of N with respect to φ^t_{LP} is given in Lindstedt-Poincaré coordinates by

$$E^s = \{(q_1, p_1, I_2, I_3, \varphi_1, \varphi_2) \in M_{\mathrm{LP}} \colon q_1 = 0\}$$
$$E^u = \{(q_1, p_1, I_2, I_3, \varphi_1, \varphi_2) \in M_{\mathrm{LP}} \colon p_1 = 0\}.$$

Notice that $E^{s,u}$ is a bundle over N.

This gives a splitting for every $x \in N$

$$T_x M_{\mathrm{LP}} = E^s_x \oplus E^u_x \oplus T_x N$$

in such a way that

$$\begin{aligned} v \in E^s_x &\Leftrightarrow |D(\varphi^t)_x v| \leq Ce^{-\lambda t}|v| \quad t \geq 0 \\ v \in E^u_x &\Leftrightarrow |D(\varphi^t)_x v| \leq Ce^{-\lambda |t|}|v| \quad t \leq 0 \\ v \in T_x N &\Leftrightarrow |D(\varphi^t)_x v| \leq C|v| \quad t \in \mathbb{R}, \end{aligned}$$

where in this case $C = 1$ and λ is given in equation (10). This is precisely the characterization of a normally hyperbolic invariant manifold. Therefore,

$$\Lambda = k(N) \tag{22}$$

is an (approximate) normally hyperbolic invariant manifold for φ^t.

The restriction $k^{s,u} : E^{s,u} \to M$ defined as $k^{s,u} = k|_{E^{s,u}}$ maps $E^{s,u}$ to

$$W^{s,u}_{\mathrm{loc}}(\Lambda) = \{k^{s,u}(x) \colon x = (q_1, p_1, I_2, I_3, \varphi_1, \varphi_2) \in E^{s,u}\} \cap V_{\mathrm{LP}}. \tag{23}$$

The local stable and unstable manifolds of a point $x = k\left(\bar{I}_2, \bar{I}_3, \bar{\varphi}_2, \bar{\varphi}_3\right) \in \Lambda$ are given by

$$\begin{aligned} W^s_{\mathrm{loc}}(x) &= \left\{k^s(y) \colon y = \left(q_1, p_1, \bar{I}_2, \bar{I}_3, \bar{\varphi}_2, \bar{\varphi}_3\right) \in M_{\mathrm{LP}},\ q_1 = 0\right\} \cap V_{\mathrm{LP}} \\ W^u_{\mathrm{loc}}(x) &= \left\{k^u(y) \colon y = \left(q_1, p_1, \bar{I}_2, \bar{I}_3, \bar{\varphi}_2, \bar{\varphi}_3\right) \in M_{\mathrm{LP}},\ p_1 = 0\right\} \cap V_{\mathrm{LP}}. \end{aligned} \tag{24}$$

4 Computation of heteroclinic trajectories

Let Λ_j (resp. Λ_i) be the normally hyperbolic invariant manifold of L_j (resp. L_i) in Hill's problem, as defined in (22). Suppose that the manifolds $W^s_{\Lambda_j}$ and $W^u_{\Lambda_i}$ intersect. If $x \in W^s_{\Lambda_j} \cap W^u_{\Lambda_i}$, then

$$\begin{aligned} \operatorname{dist}\left(\varphi^t(x), \Lambda_j\right) &\leq C_x e^{-\lambda_j t}, \quad t \geq 0 \quad \text{and} \\ \operatorname{dist}\left(\varphi^t(x), \Lambda_i\right) &\leq C_x e^{-\lambda_i |t|}, \quad t \leq 0. \end{aligned}$$

for some constants $\lambda_i, \lambda_j \geq 0$ associated to the equilibrium points L_i, L_j respectively. The trajectories $\varphi(t)$ passing through x are called *heteroclinic* because they are asymptotic to Λ_j in the future and Λ_i in the past.

In this section, we first review the numerical method used in [19] to compute heteroclinic trajectories towards a target torus in the spatial Hill's problem. Then this method is exploited to continue families of heteroclinic orbits (with respect to the amplitudes of the target torus). This gives a complete description of selected families of heteroclinic orbits. Details of the computation of heteroclinic families will be published elsewhere [1].

The intersection of the stable and unstable manifolds $W^s_{\Lambda_j}, W^u_{\Lambda_i}$ will be used in section 5.2 to compute heteroclinic channels. The heteroclinic trajectories will be used in section 5.3 to compute the scattering map.

We have to compute the heteroclinic trajectories first in order to find the scattering map. A natural question is whether the scattering map can be computed without going through the explicit construction of $W^s_{\Lambda_j}, W^u_{\Lambda_i}$, and the intersection of these manifolds. In the future we expect to simplify the computation of the scattering map using the perturbative formulas for its derivative given in [5].

4.1 Heteroclinic trajectories towards a fixed torus

Let us give an overview of the method used in [19] to compute heteroclinic trajectories to a given torus. The method uses the Lindstedt-Poincaré representation of the dynamics near L_i and L_j.

As input to the method, give a target invariant torus $\mathcal{T} = \mathcal{T}_{\bar{\alpha_3},\bar{\alpha_4}} \subset \Lambda_j$ for the heteroclinic trajectories. Let $c = C(\bar{\alpha_3}, \bar{\alpha_4})$ be the fixed Jacobian constant of the integral curves of $\mathcal{T}$, so that $\mathcal{T} \subset \Lambda^c_j$.

Example 1. For illustration, we will show some heteroclinic trajectories for the Sun-Earth system going from Λ^c_2 to a target torus $\mathcal{T}_{\bar{\alpha_3},\bar{\alpha_4}} \subset \Lambda^c_1$. The torus has amplitudes $\bar{\alpha_3} = 0.042$, $\bar{\alpha_4} = 0.13$, corresponding to a Jacobian constant $c = 4.26460693$.

- Fix a surface of section $\Sigma = \{X = 0\}$ perpendicular to the X axis of Hill's problem and located at the position of the small primary (the Earth).
- Consider $W^s_{\text{loc}}(\mathcal{T})$, the local stable manifold of $\mathcal{T}$, defined in (18a). Take a section of $W^s_{\text{loc}}(\mathcal{T})$:

  $$\mathrm{w}^s_0(\mathcal{T}) = \left\{k^s(x) \in W^s_{\text{loc}}(\mathcal{T}) : x = (\alpha_1, \alpha_2, \bar{\alpha_3}, \bar{\alpha_4}, \phi_1, \phi_2),\ \alpha_2 = \alpha_2^0\right\}$$

  with α_2^0 fixed. The section $\mathrm{w}^s_0(\mathcal{T})$ is a submanifold of $W^s_{\text{loc}}(\mathcal{T})$ transversal to the flow.

  Discretize the section $\mathrm{w}^s_0(\mathcal{T})$ into a grid of points, sampling the angles $(\phi_1, \phi_2) \in \mathbb{T}^2$ at regular intervals. This constitutes a grid of initial conditions on $W^s_{\text{loc}}(\mathcal{T})$. The solutions having these initial conditions are numerically integrated backwards in time until they reach the surface Σ. This gives a set of points $\mathrm{w}^s_1(\mathcal{T}) \subset \Sigma$, the first intersection of the stable manifold $W^s_{\text{loc}}(\mathcal{T})$ with Σ.

  Abusing notation, we will use the same name for the manifolds $\mathrm{w}^s_0(\mathcal{T}), \mathrm{w}^s_1(\mathcal{T})$ and their discrete numerical approximation.

Figure 1 illustrates (in example 1) the continuation of the stable manifold $W^s_{\mathcal{T}}$ from a set of initial conditions very close to the torus ($\alpha_2^0 = 10^{-3}$). Note that the numerically integrated orbits approximate the stable manifold $W^s_{\mathcal{T}}$. Figure 2 illustrates the set $\mathrm{w}^s_1(\mathcal{T})$.

- Similarly, consider the normally hyperbolic invariant manifold Λ^c_i restricted to the energy level c, with associated unstable manifold $W^u_{\text{loc}}(\Lambda^c_i)$. Take a section of $W^u_{\text{loc}}(\Lambda^c_i)$:

  $$\mathrm{w}^u_0(\Lambda^c_i) = \left\{k^u(x) \in W^u_{\text{loc}}(\Lambda^c_i) : x = (\alpha_1, \alpha_2, \alpha_3, \alpha_4, \phi_1, \phi_2),\ \alpha_1 = \alpha_1^0\right\}$$

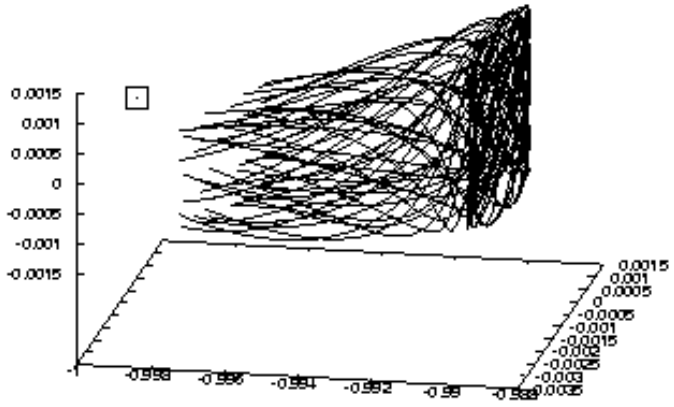

Figure 1: Continuation of $W^s_{\mathcal{T}}$, in RTBP coordinates. The torus $\mathcal{T}$ is on the right-hand side. The initial conditions are so close to the torus that they are hardly distinguishible from it. The small box marks the location of the Earth.

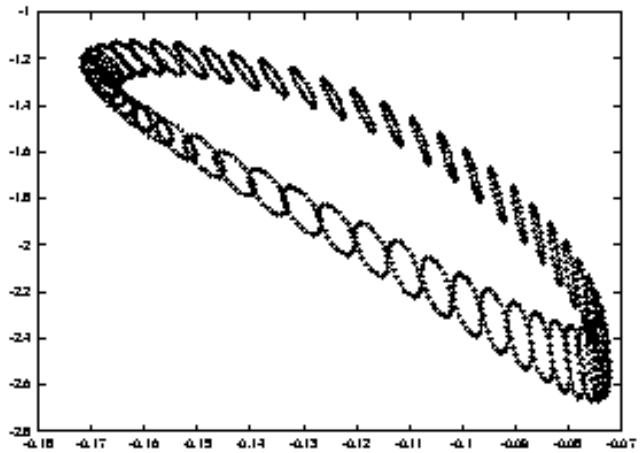

Figure 2: First intersection of $W^s_{\mathcal{T}}$ with the surface of section Σ. This set is denoted $\mathrm{w}^s_1(\mathcal{T})$ in the text. Only the $Y\dot{Y}$ projection is shown here.

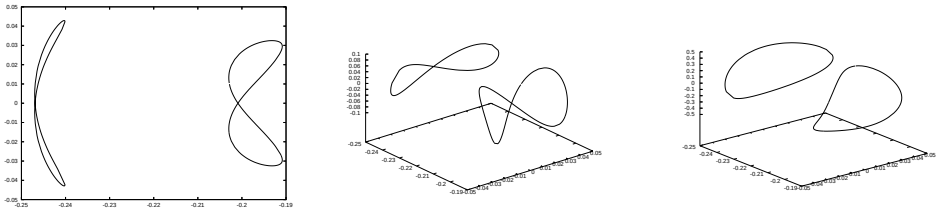

Figure 3: First nonempty intersection of $W^s_{\mathcal{T}}$ and $W^u_{\Lambda^c_2}$ restricted to the surface of section Σ. It happens after the stable and unstable manifolds have cut Σ three times. This set is denoted $\gamma^{3,3}(\mathcal{T})$ in the text. Left: YZ projection, center: $YZ\dot{Y}$ projection, right: $YZ\dot{Z}$ projection.

with α^0_1 fixed. The section $\mathrm{w}^u_0(\Lambda^c_i)$ is a submanifold of $W^u_{\mathrm{loc}}(\Lambda^c_i)$ transversal to the flow.

Discretize the section $\mathrm{w}^u_0(\Lambda^c_i)$ into a grid of points. Numerically integrate these initial conditions forward in time until they reach Σ, to obtain a set of points $\mathrm{w}^u_1(\Lambda^c_i) \in \Sigma$.

One can also compute subsequent intersections of the asymptotic manifolds with Σ as they are continued. We will denote these sets by $\mathrm{w}^s_n(\mathcal{T}) \subset \Sigma$ and $\mathrm{w}^u_n(\Lambda^c_i) \subset \Sigma$ for $n = 2, 3, 4, \ldots$.

- Look for the heteroclinic set (restricted to Σ)

$$\gamma^{m,n}(\mathcal{T}) = \mathrm{w}^s_m(\mathcal{T}) \cap \mathrm{w}^u_n(\Lambda^c_i) \subset \Sigma.$$

First look for close encounters of the discrete sets $\mathrm{w}^s_m(\mathcal{T})$ and $\mathrm{w}^u_n(\Lambda^c_i)$ using Euclidian distance.

Then, for each pair of points $(x, y) \in \mathrm{w}^s_m(\mathcal{T}) \times \mathrm{w}^u_n(\Lambda^c_i)$ candidate to an intersection, use a Newton method to find a true intersection. Specifically, let $x^0 \in \mathrm{w}^s_0(\mathcal{T})$ be the initial condition whose solution integrates to x backward in time, and let $y^0 \in \mathrm{w}^u_0(\Lambda^c_i)$ be the initial condition whose solution integrates to y forward in time. Leave x^0 fixed, and correct y^0 using a Newton method until $x = y$. This gives (a numerical approximation to) $\gamma^{m,n}(\mathcal{T})$.

If $x \in \gamma^{m,n}(\mathcal{T})$ then $x \in W^s_{\mathcal{T}} \cap W^u_{\Lambda^c_i}$, so each point $x \in \gamma^{m,n}(\mathcal{T})$ gives rise to a heteroclinic solution tending to Λ^c_i in the past and $\mathcal{T}$ in the future. A single point $x \in \gamma^{m,n}(\mathcal{T})$ is enough to recover the whole heteroclinic orbit passing through x. However, it is useful to record the following extra information associated to the orbit: the points $x^0 \in \mathrm{w}^s_0(\mathcal{T})$ and $y^0 \in \mathrm{w}^u_0(\Lambda^c_i)$, and the integration times t_s and t_u such that $\varphi^{t_s}(x) = x^0$ and $\varphi^{t_u}(y_0) = y$. Therefore, the output of the method is the set $\gamma^{m,n}(\mathcal{T})$ and, for each $x \in \gamma^{m,n}(\mathcal{T})$, the associated extra information x^0, y^0, t_s, t_u.

We will denote $\gamma^{m,n}_0(\mathcal{T})$ the trace of the heteroclinic trajectories on the section $\mathrm{w}^s_0(\mathcal{T})$:

$$\gamma^{m,n}_0(\mathcal{T}) = \left\{ x_0 \in \mathrm{w}^s_0(\mathcal{T}) : x_0 = \varphi^{t_s}(x) \text{ for some } x \in \gamma^{m,n}(\mathcal{T}) \right\}.$$

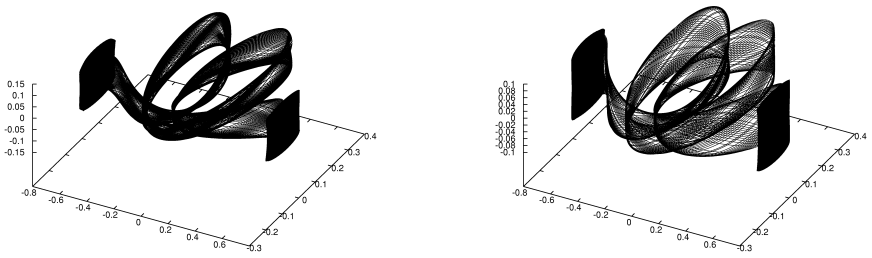

Figure 4: $\Lambda_2 - \mathcal{T}$ heteroclinic orbits generated from $\gamma^{3,3}(\mathcal{T})$. The two families correspond to the different connected components of $\gamma^{3,3}(\mathcal{T})$. All trajectories tend to $\mathcal{T} \in \Lambda_1$ (on the right-hand side of the pictures).

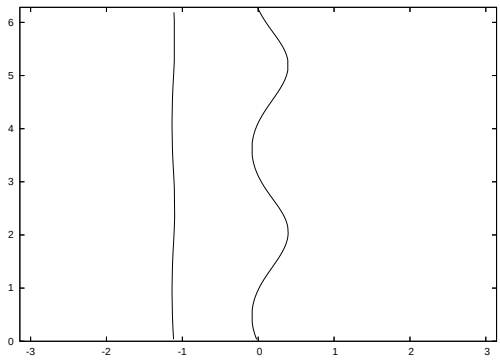

Figure 5: Projection of the heteroclinic set $\gamma^{3,3}(\mathcal{T})$ back onto the initial section of the stable manifold, $\mathrm{w}_0^s(\mathcal{T})$. Plotted are the in-plane (horizontal axis) and out-of-plane phases (vertical axis) of states $x^0 \in \mathrm{w}_0^s(\mathcal{T})$ having a heteroclinic trajectory. This set is denoted $\gamma_0^{3,3}(\mathcal{T})$ in the text.

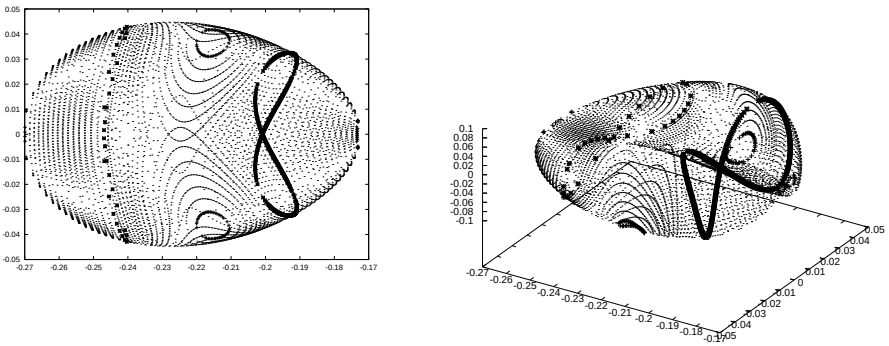

Figure 6: First nonempty intersection of $W^s_{\Lambda_1^c}$ and $W^u_{\Lambda_2^c}$ restricted to the surface of section Σ. This set is denoted $\gamma^{3,3}$ in the text. Left: YZ projection, right: $YZ\dot{Y}$ projection.

In example 1, the first nonempty intersection of $\mathrm{w}^s_m(\mathcal{T})$ and $\mathrm{w}^u_n(\Lambda_i^c)$ happens for $m = 3, n = 3$. Figure 3 shows $\gamma^{3,3}(\mathcal{T})$. Figure 4 shows the resulting heteroclinic orbits generated from $\gamma^{3,3}(\mathcal{T})$. Figure 5 shows $\gamma_0^{3,3}(\mathcal{T})$, the trace of the heteroclinic trajectories on the section $\mathrm{w}^s_0(\mathcal{T})$.

4.2 Heteroclinic trajectories from Λ_i to Λ_j

We have seen how to compute heteroclinic trajectories from Λ_i to a given torus $\mathcal{T} \subset \Lambda_j$. However, the more natural question remains to describe all heteroclinic trajectories from Λ_i to Λ_j.

Remark 2. Notice that, given $C = c$, the problem amounts to describe all heteroclinic trajectories from Λ_i^c to Λ_j^c.

Let us denote $\gamma^{m,n}$ the heteroclinic set (restricted to Σ) associated to an energy level:

$$\gamma^{m,n} = \mathrm{w}^s_m\left(\Lambda_j^c\right) \cap \mathrm{w}^u_n\left(\Lambda_i^c\right) \subset \Sigma.$$

Recall from equation (19) that the family of invariant tori Λ_j^c can be parametrized by $\alpha = \alpha_4 \in [\alpha_{min}, \alpha_{max}]$, so

$$\gamma^{m,n} = \bigcup_{\alpha \in [\alpha_{min}, \alpha_{max}]} \gamma^{m,n}(\mathcal{T}_\alpha).$$

Assume that we have already obtained a set of heteroclinic orbits to a given torus $\mathcal{T}_\alpha$ by the method of section 4.1. That is, we have obtained $\gamma^{m,n}(\mathcal{T}_\alpha)$ and associated data x^0, y^0 for each $x \in \gamma^{m,n}(\mathcal{T}_\alpha)$. The family of heteroclinic orbits can be continued with respect to the target torus $\mathcal{T}_\alpha \subset \Lambda_j^c$. Vary the amplitude $\tilde{\alpha} = \alpha + \Delta\alpha$ of the target torus and for each heteroclinic orbit, refine x^0 and y^0 using Newton's method to find a new intersection $\tilde{x} \in \gamma^{m,n}(\mathcal{T}_{\tilde{\alpha}})$.

It may happen that the asymptotic manifolds $W^s_{\mathcal{T}}$ and $W^u_{\Lambda_i}$ cease to intersect as α varies, so the heteroclinic family ceases to exist.

Let us describe the heteroclinic set $\gamma^{3,3}$ in our numerical example (energy level $c = 4.26460693$) as $\alpha = \alpha_4$ varies. The set $\gamma^{3,3}$ is represented in figure 6.

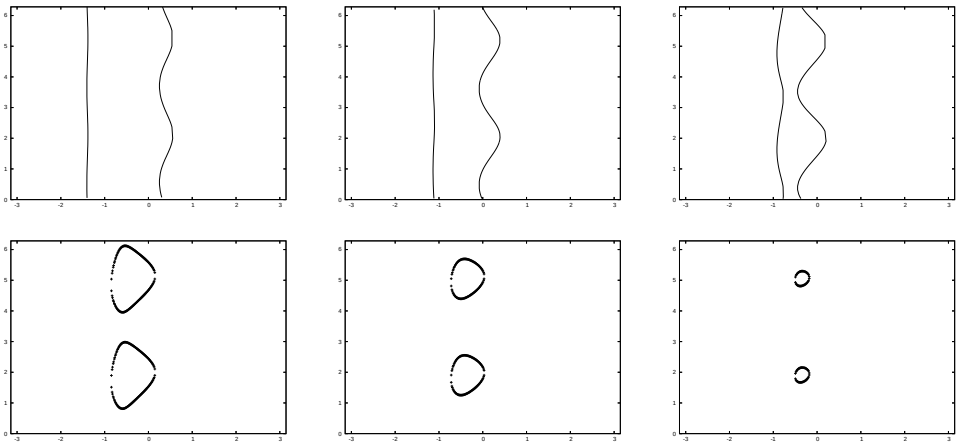

Figure 7: Evolution of the set $\gamma_0^{3,3}(\mathcal{T}_\alpha)$ on the section $\mathrm{w}_0^s(\mathcal{T}_\alpha)$ as the amplitude α of the torus varies. The pictures correspond to $\alpha = 0.0816, 0.1300, 0.1436, 0.1463, 0.1500, 0.1534$ (top to bottom and left to right).

- When $\alpha = \alpha_4 = 0$, the target torus $\mathcal{T} = \mathcal{T}_\alpha$ is a planar Lyapunov orbit, and the manifolds $W^s_{\mathcal{T}}$ and $W^u_{\Lambda_2^c}$ intersect on the surface Σ in just two points, the leftmost and rightmost points of figure 6 (YZ projection).
- As α increases, the torus $\mathcal{T}_\alpha$ has larger out-of-plane amplitude, and the manifolds intersect on Σ in two components homeomorphic to S^1. For instance, for $\alpha = \alpha_4 = 0.13$ we recover the set $\gamma^{3,3}(\mathcal{T}_\alpha)$ of section 4.1, marked with asterisks in figure 6. The trace $\gamma_0^{3,3}(\mathcal{T}_\alpha)$ of the heteroclinic orbits on $\mathrm{w}_0^s(\mathcal{T}_\alpha)$ is shown in figure 7, second picture; it is just a repetition of figure 5.
- At some critical value $\alpha = \alpha_4 \approx 0.145$, the trace $\gamma_0^{3,3}(\mathcal{T}_\alpha)$ on $\mathrm{w}_0^s(\mathcal{T}_\alpha)$ changes from two noncontractible curves to two contractible curves, as shown in figure 7, third and fourth pictures.
- Finally, as $\alpha = \alpha_4 \to 0.1799$, the manifolds cease to intersect, and $\gamma^{3,3}(\mathcal{T}_\alpha)$ collapses in two points inside the two small circles marked with crosses in figure 6. This corresponds to the last picture in figure 7.

5 Scattering map

In this section we discuss the scattering maps associated to transversal intersections of $W^s_{\Lambda_j}$ and $W^u_{\Lambda_i}$ in the spatial Hill's problem. A scattering map in this context is a map from Λ_i to Λ_j which describes in a precise sense the asymptotic behaviour of heteroclinic solutions.

The scattering map discussed in this paper is an instance of the general definition given in [5], except for the fact that ours describes heteroclinic instead of homoclinic solutions.

A crucial step is the construction of a *heteroclinic channel* (see definition (2)) through which a scattering map is defined. For the spatial Hill's problem, we give a criterion to determine heteroclinic channels (proposition 1) that is easy to check in practice. This is one of the main differences with respect to the planar RTBP, where heteroclinic channels were easier to determine [2]. As a consequence, in the spatial case the domain and range of the scattering map are not all of Λ, as they were in the planar case.

The scattering map for the spatial case relates tori of different amplitudes, allowing for more complex and interesting applications.

5.1 Wave operators

In order to have a precise description of the asymptotic behaviour of solutions in the stable and unstable manifolds, in this section we describe the wave maps, defined from the stable or unstable manifold of a normally hyperbolic invariant manifold Λ to Λ itself. We also explain how to compute them. The main reference for the general definition and properties of the wave operators and the scattering map is [5].

For a normally hyperbolic invariant manifold Λ, the assympotic manifolds of points $x \in \Lambda$ give a one-dimensional foliation of $W^{s,u}_\Lambda$:

$$W^{s,u}_\Lambda = \bigcup_{x\in\Lambda} W^{s,u}_x \qquad \text{and} \qquad W^{s,u}_x \cap W^{s,u}_y = \emptyset \quad \text{if} \quad x \neq y. \tag{25}$$

For a point $x \in W^s_\Lambda$ (resp. $x \in W^u_\Lambda$), we denote by x_+ (resp. x_-) the point in Λ such that $x \in W^s_{x_+}$ (resp. $x \in W^u_{x_-}$)

Definition 1. The projection maps defined by

$$\begin{aligned} \Omega_\pm \colon W^{s,u}_\Lambda &\to \Lambda \\ x &\to x_\pm \end{aligned}$$

are called the wave operators.

The name "wave operators", sometimes also called Møller transformations, comes from the physics litterature (see [24], for instance).

Notice that $\Omega_\pm\left(\varphi^t(x)\right) = \varphi^t(x_\pm)$ for all $x \in W^{s,u}_{x_\pm}$ and $t \in \mathbb{R}$, so the wave operators have the following invariance property:

$$\Omega_\pm = \varphi^{-t} \circ \Omega_\pm \circ \varphi^t. \tag{26}$$

We proceed to discuss the wave maps in Hill's problem. Let $\Lambda = \Lambda_1$ or Λ_2. Notice that the foliation of $W^{s,u}_{\text{loc}}(\Lambda)$ is explicit in the Lindstedt-Poincaré parametrization (23) and (24). Actually, in the Lindstedt-Poincaré approximation, we have something stronger: $W^{s,u}_{\text{loc}}(\Lambda) = \bigcup_{x\in\Lambda} W^{s,u}_x$ is a fiber bundle with base space Λ and fiber space $\mathbb{R}$, i.e. the following diagram commutes:

$$\begin{array}{ccc} W^{s,u}_{\text{loc}}(\Lambda) & \xrightarrow{(k^{s,u})^{-1}} & E^{s,u} = N \times \mathbb{R} \\ \Big\downarrow{\scriptstyle \Omega_\pm} & & \Big\downarrow{\scriptstyle \text{proj}_N} \\ \Lambda & \xleftarrow{\quad k \quad} & N \end{array}$$

where $\mathrm{proj}_N \colon N \times \mathbb{R} \to N$ is the natural projection onto N, $k \colon N \to M$ is the parametrization defined in section 3.2, and $k^{s,u} \colon E^{s,u} \to M$ are the parametrizations defined in section 3.3. The fiber over x is $W^{s,u}_{\mathrm{loc}}(x)$.

Thus, $\Omega_\pm$ is locally given by

$$\Omega_\pm|_{W^{s,u}_{\mathrm{loc}}(\Lambda)} = k \circ \mathrm{proj}_N \circ (k^{s,u})^{-1}.$$

For instance, given $x = k^s(0, p_1, I_2, I_3, \varphi_2, \varphi_3) \in W^s_{\mathrm{loc}}(\Lambda)$ in Lindstedt-Poincaré coordinates,

$$\begin{aligned} \Omega_+(x) &= k \circ \mathrm{proj}_N \circ (k^s)^{-1}(x) \\ &= k \circ \mathrm{proj}_N(0, p_1, I_2, I_3, \varphi_2, \varphi_3) \\ &= k(I_2, I_3, \varphi_2, \varphi_3). \end{aligned} \tag{27}$$

To extend $\Omega_\pm$ to the global assymptotic manifolds $W^{s,u}_\Lambda$, one has to combine the semianalytical expression (27) with purely numerical techniques. Recall from section 4 that $\mathrm{w}^s_0(\Lambda)$ denotes a section of the local stable manifold $W^s_{\mathrm{loc}}(\Lambda)$. Given a point $x \in W^s_\Lambda$ far from Λ, one can numerically integrate the solution $\varphi(t, x)$ until it reaches the section $\mathrm{w}^s_0(\Lambda)$ at a point

$$x^0 = \varphi(t_s, x) \in \mathrm{w}^s_0(\Lambda),$$

where $t_s = t_s(x)$ depends on x.

As $x^0 \in W^s_{\mathrm{loc}}(\Lambda)$, we can compute $x^0_+ = \Omega_+(x^0)$ using expression (27): if $x^0 = k^s\left(0, p^0_1, I^0_2, I^0_3, \varphi^0_2, \varphi^0_3\right)$, then $x^0_+ = k\left(I^0_2, I^0_3, \varphi^0_2, \varphi^0_3\right)$. Then, using invariance property (26),

$$\Omega_+(x) = \Omega_+(\varphi^{-t_s}(x^0)) = \varphi^{-t_s}(x^0_+).$$

Finally, using the conjugacy (16) and equations (21) for the solution we obtain

$$\begin{aligned} \Omega_+(x) &= \varphi^{-t_s}\left(k\left(I^0_2, I^0_3, \varphi^0_2, \varphi^0_3\right)\right) \\ &= k\left(\varphi^{-t_s}_{\mathrm{LP}}\left(I^0_2, I^0_3, \varphi^0_2, \varphi^0_3\right)\right) \\ &= k\left(I^0_2, I^0_3, \varphi^0_2 - \omega t_s, \varphi^0_3 - \nu t_s\right). \end{aligned} \tag{28}$$

Similarly for the unstable manifold, given $y \in W^u_\Lambda$ far from Λ and $y^0 = \varphi(-t_u, y) = k^u\left(q^0_1, 0, I^0_2, I^0_3, \varphi^0_2, \varphi^0_3\right) \in \mathrm{w}^u_0(\Lambda)$,

$$\Omega_-(y) = k\left(I^0_2, I^0_3, \varphi^0_2 + \omega t_u, \varphi^0_3 + \nu t_u\right). \tag{29}$$

From (28) and (29) it is clear that the wave map in Lindstedt-Poincaré coordinates is just a translation by the linear flow on the target torus. Notice that the translation is not uniform, because t_s (resp. t_u) depends on the point x (resp. y).

Remark 3. Let us illustrate the action of the wave operator in our numerical example (example 1). Take for instance the heteroclinic set $\gamma^{3,3}(\mathcal{T}) \subset \Sigma$, depicted in figure 3. Integrating this set numerically up to $\mathrm{w}^s_0(\Lambda_1)$ we would recover the set $\gamma^{3,3}_0(\mathcal{T})$ (figure 5). The image under the positive wave map $\gamma^{3,3}_+(\mathcal{T}) = \Omega_+\left(\gamma^{3,3}(\mathcal{T})\right)$ would be a (nonuniform) translation of $\gamma^{3,3}_0(\mathcal{T})$ by the linear flow on the torus $\mathcal{T}$.

5.2 Heteroclinic channels

A heteroclinic channel is a restriction of a heteroclinic manifold to a submanifold where the wave operators are diffeomorphisms. The invertibility of the wave operators will be needed in section 5.3 to define the scattering map.

Given two normally hyperbolic invariant manifolds Λ_i, Λ_j of the same dimension, let $\Gamma \subset W^s_{\Lambda_j} \cap W^u_{\Lambda_i}$ be a heteroclinic manifold such that $\forall x \in \Gamma$:

$$T_x M = T_x W^s_{\Lambda_j} + T_x W^u_{\Lambda_i} \tag{30a}$$

$$T_x W^s_{\Lambda_j} \cap T_x W^u_{\Lambda_i} = T_x \Gamma. \tag{30b}$$

We then say that $W^s_{\Lambda_j}$ and $W^u_{\Lambda_i}$ intersect transversally along Γ.

Under condition (30), it is not hard to see that the dimension of Γ has to be equal to the dimension of $\Lambda_{i,j}$. As a consequence, for all $x \in \Gamma$

$$T_x \Gamma \oplus T_x W^s_{x_+} = T_x W^s_{\Lambda_j} \tag{31a}$$

$$T_x \Gamma \oplus T_x W^u_{x_-} = T_x W^u_{\Lambda_i}. \tag{31b}$$

We then say that Γ is transversal to the $\{W^s_x\}_{x\in\Lambda_j}, \{W^u_x\}_{x\in\Lambda_i}$ foliation.

Given a manifold Γ verifying condition (30), we may consider the wave operators $\Omega_\pm$ restricted to Γ. Denote $\Omega^\Gamma_\pm = \Omega_\pm|_\Gamma$, and $H^\Gamma_\pm = \Omega_\pm(\Gamma) \subset \Lambda_{j,i}$, so that

$$\Omega^\Gamma_\pm \colon \Gamma \to H^\Gamma_\pm.$$

Condition (31) guarantees that $\Omega^\Gamma_\pm$ are local diffeomorphisms in a neighbourhood of each $x \in \Gamma$. Restricting Γ if necessary, $\Omega^\Gamma_\pm$ are diffeomorphisms and in such case, we introduce the definition of a heteroclinic channel.

Definition 2. We say that Γ is a heteroclinic channel if:

1. $\Gamma \subset W^s_{\Lambda_j} \cap W^u_{\Lambda_i}$ verifies (30).
2. The wave operators $\Omega^\Gamma_\pm \colon \Gamma \to H^\Gamma_\pm$ are diffeomorphisms.

This definition is analogous to the definition given in [5] for a homoclinic channel.

Remark 4. Note that if Γ is a heteroclinic channel, so is $\varphi^t(\Gamma)$ for any $t \in \mathbb{R}$.

It is also not hard to show the following conjugation properties (see [5]). For any $t \in \mathbb{R}$,

$$\Omega^\Gamma_+ = \varphi^{-t} \circ \Omega^{\varphi^t(\Gamma)}_+ \circ \varphi^t \tag{32a}$$

$$\Omega^\Gamma_- = \varphi^{t} \circ \Omega^{\varphi^{-t}(\Gamma)}_- \circ \varphi^{-t}. \tag{32b}$$

Let us discuss next the heteroclinic channels in Hill's problem. Recall that the phase space M is 6-dimensional, $\Lambda_{1,2}$ are 4-dimensional and $E^{s,u}_x$ are 1-dimensional for any $x \in M$. Thus $W^{s,u}_x$ are also 1-dimensional, and $W^s_{\Lambda_j}, W^u_{\Lambda_i}$ are 5-dimensional. Under condition (30) we would have $\dim \Gamma = \dim \Lambda_{1,2} = 4$.

Λ_1, Λ_2 decompose into energy level sets Λ^c_1, Λ^c_2 (remark 2) that are normally hyperbolic invariant manifolds in the energy restricted phase space M^c, so it is enough to consider heteroclinic channels from Λ^c_i to Λ^c_j for any given

c. Notice that the energy restricted phase space M^c is 5-dimensional, $\Lambda^c_{1,2}$ are 3-dimensional, and $W^s_{\Lambda^c_j}$ and $W^u_{\Lambda^c_i}$ are 4-dimensional. Let us denote Γ^c an energy restricted heteroclinic channel: $\Gamma^c = \Gamma \cap M^c$. Under condition (30) we have that $\dim \Gamma^c = \dim \Lambda^c_{1,2} = 3$.

As we did in section 4, we take the global Poincaré section $\Sigma = \{X = 0\}$ to reduce the dimension of the problem. Given a heteroclinic channel Γ^c and a section Σ, let γ be the heteroclinic manifold

$$\gamma = \gamma^c = \Gamma^c \cap \Sigma,$$

and define $\Omega^\gamma_\pm = \Omega_\pm|_\gamma$, $h^\gamma_\pm = \Omega_\pm(\gamma) \subset H^{\Gamma^c}_\pm$. Note that $\dim \gamma = \dim \Gamma^c - 1$, and $\dim h^\gamma_\pm = \dim H^{\Gamma^c}_\pm - 1$. Then we have that $\Omega^\gamma_\pm \colon \gamma \to h^\gamma_\pm$ is a diffeomorphism. We have called γ a *reduced heteroclinic channel* associated to Γ^c, and $\Omega^\gamma_\pm$ a *reduced wave operator*.

Indeed, in section 4 we have already computed reduced heteroclinic manifolds $\gamma^{m,n}$ that will give rise to reduced wave operators, as explained below. The following remark is used to compute the wave operators $\Omega^{\Gamma^c}_\pm$ from the reduced wave operators $\Omega^\gamma_\pm$.

Remark 5. Given $\tilde{x} \in \Gamma^c$, suppose we were to compute $\Omega^{\Gamma^c}_\pm(\tilde{x})$. Find t such that the image of $\tilde{x}$ under the t-flow lies on the section Σ, and introduce $x = \varphi^t(\tilde{x}) \in \gamma$. Then, using property (32),

$$\Omega^{\Gamma^c}_\pm(\tilde{x}) = \varphi^{-t} \circ \Omega^{\varphi^t(\Gamma^c)}_\pm(x) = \varphi^{-t} \circ \Omega^\gamma_\pm(x) \tag{33}$$

so the problem amounts to determine the reduced wave operator $\Omega^\gamma_\pm$.

Therefore, our strategy will be to define $\Omega_\pm$ on a reduced channel γ, choosing γ carefully in such a way that $\Omega^\gamma_\pm \colon \gamma \to h^\gamma_\pm$ can be extended into a diffeomorphism $\Omega^{\Gamma^c}_\pm \colon \Gamma^c \to H^{\Gamma^c}_\pm$.

Remark 6. In analogy with complex analysis, $\Omega^{\Gamma^c}_\pm$ can be seen as a branch of the multivalued function $\Omega_\pm$. The branch of $\Omega_\pm(x)$ is chosen in reference to its specific value on Σ, namely $\Omega^\gamma_\pm(x)$.

Recall from equation (19) that, in the Lindstedt-Poincaré approximation, the normally hyperbolic invariant manifold Λ^c_j if foliated by invariant tori. To further reduce the dimension of the problem, we first look for heteroclinic manifolds (restricted to Σ) towards a given torus $\mathcal{T} = \mathcal{T}_\alpha \subset \Lambda^c_j$

$$\gamma(\mathcal{T}) \subset (W^s_{\mathcal{T}} \cap \Sigma) \cap \left(W^u_{\Lambda^c_i} \cap \Sigma\right)$$

such that the extended heteroclinic manifold

$$\Gamma^c(\mathcal{T}) = \left\{\varphi^t(\gamma(\mathcal{T})) : t \in (-\epsilon, \epsilon)\right\} \tag{34}$$

verifies

$$\forall x \in \gamma(\mathcal{T}) \qquad T_x\Gamma^c(\mathcal{T}) \oplus T_x W^s_{x_+} = T_x W^s_{\mathcal{T}}. \tag{35}$$

Consider one of the heteroclinic sets $\gamma^{m,n}(\mathcal{T}) = \mathrm{w}^s_m(\mathcal{T}) \cap \mathrm{w}^u_n(\Lambda^c_i) \subset \Sigma$ introduced in section 4.1. We look for $\gamma(\mathcal{T})$ as 1-dimensional heteroclinic manifolds inside $\gamma^{m,n}(\mathcal{T})$.

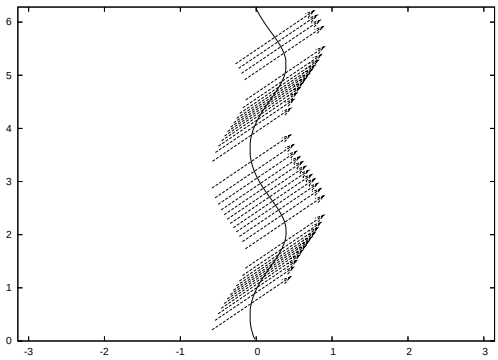

Figure 8: Illustration of proposition 1. The target torus corresponds to $c = 4.26460693$ and $\bar{\alpha_4} = 0.13$. The set $\gamma_+(\mathcal{T})$ is represented as a continuous line. The flow on the torus is represented with discontinuous arrows of slope ν/ω. The coordinates are the in-plane angle ϕ_1 (horizontal) and the out-of-plane angle ϕ_2.

Proposition 1. *Let $\gamma(\mathcal{T}) \subset \gamma^{m,n}(\mathcal{T})$ be a heteroclinic manifold with extended heteroclinic manifold $\Gamma^c(\mathcal{T})$, and consider the set $\gamma_+(\mathcal{T}) = \Omega_+(\gamma(\mathcal{T})) \subset \mathcal{T}$, which is just a curve on $\mathcal{T}$ (see remark 3). Let $x \in \gamma(\mathcal{T})$ and $x_+ = \Omega_+(x) \in \gamma_+(\mathcal{T})$.*

Assume that the target torus $\mathcal{T}$ has associated in-plane and out-of-plane frequencies ω, ν. Then, condition (35) is verified at $x \in \gamma(\mathcal{T})$ if and only if

Condition C *the slope of the curve $\gamma_+(\mathcal{T})$ (in the angular coordinates ϕ_1, ϕ_2) at the point x_+ is different from $\frac{\nu}{\omega}$.*

Proof. We assume that $\Gamma^c(\mathcal{T})$ is near $\mathcal{T}$; if it is not, one can always transport $\Gamma^c(\mathcal{T})$ by the flow towards $\mathcal{T}$ and prove it there, because property (35) is invariant under diffeomorphisms. Therefore we can use Lindstedt-Poincaré coordinates to describe the spaces $T_x\Gamma^c(\mathcal{T}), T_xW^s_{x_+}$ and $T_xW^s_{\mathcal{T}}$ involved in the proof.

The proof consists in writting $\Gamma^c(\mathcal{T})$ and $W^s_{x_+}$ in these coordinates and studying whether they intersect transversally at the point $x \in \gamma(\mathcal{T})$. Expressing $\Gamma^c(\mathcal{T})$ in terms of $\gamma_+(\mathcal{T})$, we obtain that condition (35) is equivalent to the assertion that the tangent vectors $T_{x_+}\gamma_+(\mathcal{T})$ and $T_{x_+}\text{Orbit}(x_+)$ are not parallel. Since the slope of Orbit (x_+) on $\mathcal{T}$ is ν/ω, we get the result. □

The proposition is of course also true for the unstable foliation.

We remark that the characterization given in proposition 1 is very easy to check, even visually. Take for instance our numerical example (example 1). Given $c = 4.26460693$ and $\bar{\alpha_4} = 0.13$, we have already computed $\gamma^{3,3}(\mathcal{T})$ (figure 3). Let $\gamma(\mathcal{T}) \subset \gamma^{3,3}(\mathcal{T})$ be the heteroclinic manifold consisting of one of the connected components of $\gamma^{3,3}(\mathcal{T})$, and consider the set $\gamma_+(\mathcal{T})$, represented as a continuous line in figure 8. The target torus has associated frequencies $(\omega, \nu) = (2.06930834, 1.99773353)$. The flow on the torus is represented with discontinuous lines of slope $\nu/\omega = 0.96541123$. The slope of $\gamma_+(\mathcal{T})$ is different from ν/ω at every $x_+ \in \gamma_+(\mathcal{T})$. According to proposition 1, there exists a local

extension $\Gamma^c(\mathcal{T})$ of $\gamma(\mathcal{T})$ on which condition (35) is verified. Therefore, $\Omega_+^{\Gamma^c(\mathcal{T})}$ is a local diffeomorphism in a neighborhood of x for all $x \in \gamma(\mathcal{T})$.

$\Omega_+^{\gamma(\mathcal{T})}\colon \gamma(\mathcal{T}) \to h_+^{\gamma(\mathcal{T})}$ is a diffeomorphism, where $h_+^{\gamma(\mathcal{T})} = \gamma_+(\mathcal{T})$. By the above argument, it extends to a diffeomorphism $\Omega_+^{\Gamma^c(\mathcal{T})}\colon \Gamma^c(\mathcal{T}) \to H_+^{\Gamma^c(\mathcal{T})}$, where $\Gamma^c(\mathcal{T})$ is defined in (34), and $H_+^{\Gamma^c(\mathcal{T})} = \Omega_+(\Gamma^c(\mathcal{T}))$.

Note that, using definition (34) and property (26),

$$H_+^{\Gamma^c(\mathcal{T})} = \left\{\varphi^t\left(h_+^{\gamma(\mathcal{T})}\right) : t \in (-\epsilon, \epsilon)\right\}. \tag{36}$$

$H_+^{\Gamma^c(\mathcal{T})}$ would be a band around $\gamma_+(\mathcal{T})$ represented by the arrows in figure 8.

Clearly, ϵ must be taken sensibly less than 2π in expression (36) to avoid autointersections with $h_+^{\gamma(\mathcal{T})}$. That is, $H_+^{\Gamma^c(\mathcal{T})}$ can not be extended indefinitely by the flow because of the lack of monodromy.

Actually, due to remark 5, we can compute $\Omega_+^{\Gamma^c(\mathcal{T})}$ from $\Omega_+^{\gamma(\mathcal{T})}$. Condition C guarantees that the curve $\gamma_+(\mathcal{T})$ is really a Poincaré section for the flow φ^t on the torus $\mathcal{T}$, so that $\Omega_\pm^{\Gamma^c}(\tilde{x}) = \varphi^{-t}\left(\Omega_\pm^{\gamma}(x)\right)$ is well defined in equation (33).

Remark 7. Of course, we could have chosen the other connected component of $\gamma^{3,3}(\mathcal{T})$ as the heteroclinic manifold $\gamma(\mathcal{T})$. This would give a different diffeomorphism $\Omega_+^{\Gamma^c(\mathcal{T})}$.

For all tori with amplitudes in the range $\alpha = \alpha_4 \in (0, 0.145)$, one can easily check that the heteroclinic manifolds $\gamma(\mathcal{T})$ defined in this way verify the characterization given in proposition 1. See figure 7. In all cases, the slope ω/ν is very close to 1.

Naturally, we now let

$$\gamma = \bigcup_{\alpha\in(0,0.145)} \gamma(\mathcal{T}_\alpha)$$

to obtain a heteroclinic manifold γ such that $\Omega_+^{\gamma}\colon \gamma \to h_+^{\gamma}$ is a diffeomorphism. The manifold γ has been constructed in such a way that, if we let

$$\Gamma^c = \bigcup_{\alpha\in(0,0.145)} \Gamma^c(\mathcal{T}_\alpha)$$
$$H_+^{\Gamma^c} = \bigcup_{\alpha\in(0,0.145)} H_+^{\Gamma^c(\mathcal{T}_\alpha)},$$

then $\Omega_+^{\Gamma^c}\colon \Gamma^c \to H_+^{\Gamma^c}$ is a diffeomporphism.

Up to this point, we have determined a heteroclinic manifold Γ^c on which the positive wave operator is a diffeomorphism. Similarly one could restrict Γ^c (if necessary) so that the negative wave operator is also a diffeomorphism on Γ^c. In that case, Γ^c is a heteroclinic channel, and γ is a reduced heteroclinic channel.

As we can choose between two different connected components of $\gamma^{3,3}(\mathcal{T})$, there are two possible continuous families $\gamma = \cup_\alpha \gamma(\mathcal{T}_\alpha)$, i.e. two possible heteroclinic channels.

Let us now apply proposition 1 to a torus with amplitude $\alpha = \alpha_4 = 0.15$ (see figure 7). Let $\gamma(\mathcal{T}) \subset \gamma^{3,3}(\mathcal{T})$ be the heteroclinic manifold consisting of one of the connected components of $\gamma^{3,3}(\mathcal{T})$, and consider the set $\gamma_+(\mathcal{T})$, represented

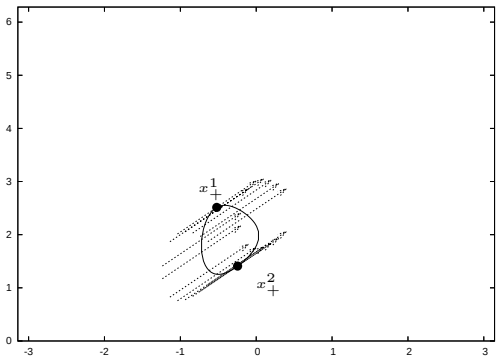

Figure 9: The target torus corresponds to $c = 4.26460693$ and $\bar{\alpha_4} = 0.15$. The set $\gamma_+(\mathcal{T})$ is represented with a continuous line. The flow on the torus is represented with discontinuous arrows of slope ν/ω. Condition C of proposition 1 is violated at the points x_+^1 and x_+^2.

with a continuous line in figure 9. The target torus has associated frequencies $(\omega, \nu) = (2.07043339, 1.99668167)$. The curve $\gamma_+(\mathcal{T})$ is tangent to the flow ν/ω at two points $x_+^1, x_+^2 \in \gamma_+(\mathcal{T})$. According to proposition 1, we have to exclude the corresponding two points x^1, x^2 from $\gamma(\mathcal{T})$.

These two points x^1, x^2 divide $\gamma(\mathcal{T})$ in two connected components. We have to further restrict the heteroclinic manifold $\gamma(\mathcal{T})$ to one of these two connected components, to avoid the lack of monodromy when $h_+^{\gamma(\mathcal{T})}$ is extended to $H_+^{\Gamma^c(\mathcal{T})}$. In this case, there are 4 possible choices for $\gamma\left(\mathcal{T}\right) \subset \gamma^{3,3}\left(\mathcal{T}\right)$.

We let

$$\gamma = \bigcup_{\alpha \in (0.145, 1.799)} \gamma\left(\mathcal{T}_\alpha\right)$$

to obtain 4 possible reduced heteroclinic channels that extend properly to heteroclinic channels.

5.3 Scattering map

Next we recall the definition of the scattering map associated to a heteroclinic channel as given in [5].

Definition 3. Given Γ a heteroclinic channel, and $\Omega_\pm^\Gamma \colon \Gamma \to H_\pm^\Gamma$ the associated wave operators, we define the scattering map associated to Γ

$$\sigma^\Gamma : H_-^\Gamma \to H_+^\Gamma$$

by

$$\sigma^\Gamma = \Omega_+^\Gamma \circ (\Omega_-^\Gamma)^{-1}.$$

Equivalently, given $x_- \in \Lambda_i$ and $x_+ \in \Lambda_j$, we write $x_+ = \sigma^\Gamma(x_-)$ whenever there exists a point $x \in \Gamma$ such that

$$\operatorname{dist}\left(\varphi^t(x), \varphi^t(x_\pm)\right) \to 0 \qquad \text{as } t \to \pm\infty.$$

Heuristically, the motion of x sincronizes with that of x_+ (and x_-) in the future (in the past).

Let $\sigma^{\Gamma,\varphi^t}$ denote the scattering map σ^Γ associated to the flow φ^t. In [5] it is shown that

$$\sigma^{\Gamma,\varphi^t} = \left(\sigma^{\Gamma,\varphi^{-t}}\right)^{-1}.$$

In applications, it is common to work with both the forward-time scattering map $\sigma^{\Gamma,\varphi^t}$ and the backward-time scattering map $\sigma^{\Gamma,\varphi^{-t}}$. For them to be defined, Ω_+^Γ and Ω_-^Γ must be invertible. This is guaranteed by the definition of heteroclinic channel (definition 2).

Recall from section 5.2 that, due to the existence of a global section for heteroclinic connections in Hill's problem, we may encode the wave operators $\Omega_\pm^\Gamma$ in the reduced wave operators $\Omega_\pm^\gamma$. They induce a reduced scattering map in the obvious way. Given a reduced heteroclinic channel γ, and $\Omega_\pm^\gamma$ the associated reduced wave operators, we define the *reduced scattering map* associated to γ, $\sigma^\gamma \colon h_-^\gamma \to h_+^\gamma$, by $\sigma^\gamma = \Omega_+^\gamma \circ \left(\Omega_-^\gamma\right)^{-1}$.

Finally, let us briefly explain how to use the scattering map in an example application to space mission design. Suppose we want to transfer a spacecraft from a given Lissajous orbit with small out-of-plane amplitude $\alpha_4 = a$ around L_1 to a Lissajous orbit with the largest possible amplitude $\alpha_4 = b$ around L_1 at the minimum fuel cost. The orbits lie on 2-dimensional invariant tori $\mathcal{T}_a \subset \Lambda_1$ resp. $\mathcal{T}_b \subset \Lambda_1$. We can solve this problem by studying the composition of a scattering map $\sigma_{12} \colon \Lambda_1 \to \Lambda_2$ and a scattering map $\sigma_{21} \colon \Lambda_2 \to \Lambda_1$.

Given heteroclinic channels

$$\begin{aligned} &\Gamma_{12} \subset W^s_{\Lambda_2} \cap W^u_{\Lambda_1} \quad \text{and} \\ &\Gamma_{21} \subset W^s_{\Lambda_1} \cap W^u_{\Lambda_2}, \end{aligned}$$

consider the associated scattering maps

$$\begin{aligned} \sigma^{\Gamma_{12}} &\colon H_-^{\Gamma_{12}} \subset \Lambda_1 \to H_+^{\Gamma_{12}} \subset \Lambda_2 \\ \sigma^{\Gamma_{21}} &\colon H_-^{\Gamma_{21}} \subset \Lambda_2 \to H_+^{\Gamma_{21}} \subset \Lambda_1. \end{aligned}$$

Define the composition map $F \colon H_-^{\Gamma_{12}} \subset \Lambda_1 \to H_+^{\Gamma_{21}} \subset \Lambda_1$ by

$$F = \sigma^{\Gamma_{21}} \circ \sigma^{\Gamma_{12}}.$$

Let $x_- = k(\alpha_3, \alpha_4 = a, \phi_1, \phi_2) \in \mathcal{T}_a$, and $x_+ = k(\alpha_3, \alpha_4 = b, \phi_1, \phi_2) \in \mathcal{T}_b$. Notice that if $F(x_-) = x_+$ then there is a transfer from $\mathcal{T}_a$ to $\mathcal{T}_b$ at almost zero cost. Thus the problem can be formulated in terms of maximizing the amplitude difference $|b - a|$ with respect to the point $x_- \in \mathcal{T}_a$ using the function F.

In the future, we plan to use the scattering map sistematically in similar applications.

Acknowledgements

This work has been supported by the MCyT-FEDER Grants BFM2003-9504 and MTM2006-00478.

References

[1] L. Arona and J.J. Masdemont. A methodology for the computation of heteroclinic orbits between invariant tori about L_1 and L_2 in the sun-earth system. *Proceedings of the AIMS Conference, Poitiers*, 2006, submitted.

[2] E. Canalias, A. Delshams, J.J. Masdemont, and P. Roldán. The scattering map in the planar restricted three body problem. *Celestial Mech. Dynam. Astronom.*, 95:155–171, 2006.

[3] C. C. Conley. Low energy transit orbits in the restricted three-body problem. *SIAM J. Appl. Math.*, 16:732–746, 1968.

[4] A. Delshams, R. de la Llave, and T.M. Seara. A geometric mechanism for diffusion in Hamiltonian systems overcoming the large gap problem: heuristics and rigorous verification on a model. *Mem. Amer. Math. Soc.*, 2005, in press.

[5] A. Delshams, R. de la Llave, and T.M. Seara. Geometric properties of the scattering map of a normally hyperbolic invariant manifold. *http://www.ma.utexas.edu/mp_arc/c/06/06-184.pdf*, 2006, preprint.

[6] Amadeu Delshams, Rafael de la Llave, and Tere M. Seara. A geometric approach to the existence of orbits with unbounded energy in generic periodic perturbations by a potential of generic geodesic flows of $\mathbf{T}^2$. *Comm. Math. Phys.*, 209(2):353–392, 2000.

[7] Amadeu Delshams and Pere Gutiérrez. Estimates on invariant tori near an elliptic equilibrium point of a Hamiltonian system. *J. Differential Equations*, 131(2):277–303, 1996.

[8] Neil Fenichel. Persistence and smoothness of invariant manifolds for flows. *Indiana Univ. Math. J.*, 21:193–226, 1971/1972.

[9] Neil Fenichel. Asymptotic stability with rate conditions. *Indiana Univ. Math. J.*, 23:1109–1137, 1973/74.

[10] G. Gómez, À. Jorba, C. Simó, and J. Masdemont. *Dynamics and mission design near libration points. Vol. III*, volume 4 of *World Scientific Monograph Series in Mathematics*. World Scientific Publishing Co. Inc., River Edge, NJ, 2001. Advanced methods for collinear points.

[11] G. Gómez, À. Jorba, C. Simó, and J. Masdemont. *Dynamics and mission design near libration points. Vol. IV*, volume 5 of *World Scientific Monograph Series in Mathematics*. World Scientific Publishing Co. Inc., River Edge, NJ, 2001. Advanced methods for triangular points.

[12] G. Gómez, J. Llibre, R. Martínez, and C. Simó. *Dynamics and mission design near libration points. Vol. I*, volume 2 of *World Scientific Monograph Series in Mathematics*. World Scientific Publishing Co. Inc., River Edge, NJ, 2001. Fundamentals: the case of collinear libration points, With a foreword by Walter Flury.

[13] G. Gómez, M. Marcote, and J. M. Mondelo. The invariant manifold structure of the spatial Hill's problem. *Dyn. Syst.*, 20(1):115–147, 2005.

[14] G. Gómez, C. Simó, J. Llibre, and R. Martínez. *Dynamics and mission design near libration points. Vol. II*, volume 3 of *World Scientific Monograph Series in Mathematics*. World Scientific Publishing Co. Inc., River Edge, NJ, 2001. Fundamentals: the case of triangular libration points.

[15] M. W. Hirsch, C. C. Pugh, and M. Shub. *Invariant manifolds*. Springer-Verlag, Berlin, 1977.

[16] Morris W. Hirsch and Charles C. Pugh. Stable manifolds and hyperbolic sets. In *Global Analysis (Proc. Sympos. Pure Math., Vol. XIV, Berkeley, Calif., 1968)*, pages 133–163. Amer. Math. Soc., Providence, R.I., 1970.

[17] Àngel Jorba. A methodology for the numerical computation of normal forms, centre manifolds and first integrals of Hamiltonian systems. *Experiment. Math.*, 8(2):155–195, 1999.

[18] Àngel Jorba and Josep Masdemont. Dynamics in the center manifold of the collinear points of the restricted three body problem. *Phys. D*, 132(1-2):189–213, 1999.

[19] J. J. Masdemont. High-order expansions of invariant manifolds of libration point orbits with applications to mission design. *Dyn. Syst.*, 20(1):59–113, 2005.

[20] Yakov B. Pesin. *Lectures on partial hyperbolicity and stable ergodicity*. Zurich Lectures in Advanced Mathematics. European Mathematical Society (EMS), Zürich, 2004.

[21] David L. Richardson. A note on a Lagrangian formulation for motion about the collinear points. *Celestial Mech.*, 22(3):231–236, 1980.

[22] C. Simó and T. J. Stuchi. Central stable/unstable manifolds and the destruction of KAM tori in the planar Hill problem. *Phys. D*, 140(1-2):1–32, 2000.

[23] V. Szebehely. *Theory of orbits*. Academic Press, 1967.

[24] Walter Thirring. *A course in mathematical physics. Vol. I. Classical dynamical systems*. Springer-Verlag, New York, 1978.